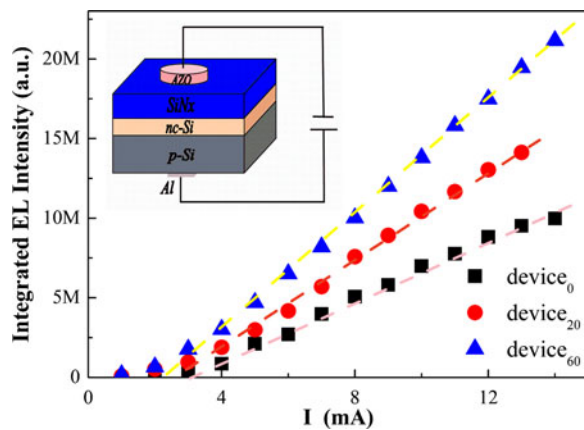


Enhanced Electroluminescence Efficiency in Si-Nanostructure-Based Silicon-Nitride Light-Emitting Diodes via H₂ Plasma Treatment

Volume 10, Number 2, April 2018

Zhenxu Lin
Yi Zhang
Wenxing Zhang
Jie Song
Hongliang Li
Chao Song
Yanqing Guo
Rui Huang



Enhanced Electroluminescence Efficiency in Si-Nanostructure-Based Silicon-Nitride Light-Emitting Diodes via H₂ Plasma Treatment

Zhenxu Lin, Yi Zhang, Wenxing Zhang , Jie Song, Hongliang Li, Chao Song, Yanqing Guo, and Rui Huang 

School of Materials Science and Engineering, Hanshan Normal University, Chaozhou 521041, China

DOI:10.1109/JPHOT.2018.2818194

1943-0655 © 2018 IEEE. Translations and content mining are permitted for academic research only.
Personal use is also permitted, but republication/redistribution requires IEEE permission. See
http://www.ieee.org/publications_standards/publications/rights/index.html for more information.

Manuscript received February 9, 2018; revised March 14, 2018; accepted March 19, 2018. Date of publication March 22, 2018; date of current version April 3, 2018. This work was supported in part by the National Natural Science Foundation of China under Grants 61274140 and 61306003; in part by the Natural Science Foundation of Guangdong Province under Grant 2015A030313871; and in part by the Young Talents in Higher Education of Guangdong, China, 2017. Corresponding author: R. Huang (e-mail: rhuangnju@126.com).

Abstract: The improved performance of Si quantum dot-based silicon nitride light-emitting devices with the inserted hole-blocking nc-Si layer was investigated. An enhanced electroluminescence (EL) efficiency of 200% from the SiN_x-based LEDs is demonstrated through H₂ plasma treatment of the inserted nc-Si layer. The enhancement of an EL efficiency is depended on time for plasma treatment. Moreover, the injected current of the devices with H₂ plasma treatment is significantly higher than that of the device without H₂ plasma treatment under the same driving voltage. The Z-parameter of the devices increases from 1.25 to 1.41 after H₂ plasma treatment of inserted nc-Si layer. The inserted nc-Si layers with and without H₂ plasma treatment were further investigated by the Raman spectroscopy and the Fourier transform infrared absorption spectroscopy, respectively. It is suggested that the improved EL efficiency is due to the suppression of nonradiative recombination, which resulted from the hydrogen passivation that effectively reducing Si-related defect states of the inserted nc-Si layer.

Index Terms: Silicon nitride, electroluminescence, H₂ plasma treatment, nanocrystalline (nc)-Si layer.

1. Introduction

Realizing an efficient Si-based light source on the mass-produced Si chips is one of the key challenges in the future microelectronic and communication technology. Among the approaches used to fabricate high-performance Si-based LEDs, silicon nanostructures embedded in silicon oxide matrix received attention because of its excellent photoluminescence (PL) and optical gain [1]–[8]. However, this system faces difficulty in efficient electrical injection, which results from high potential barrier of SiO₂ matrix (9 eV). By comparison, Si₃N₄ features lower band gap (5 eV) than SiO₂, this lower band gap can significantly improve carrier injection, resulting in effective electroluminescence (EL) at low driving voltage from SiN_x-based LEDs [9]–[16]. In Si/SiNx-based LEDs, light-emitting efficiency is limited by nonradiative recombination originating from defects in

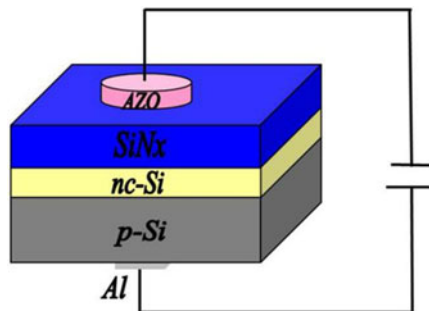


Fig. 1. Schematic diagram of the SiNx-based LED structure.

SiNx and imbalanced carrier injection, which is caused by asymmetric band offset between SiN_x and Si nanostructure. To achieve highly efficient Si/SiN_x-based LEDs, various methods were devoted to overcome above mentioned problems. To balance injection of electron and hole, nc-Si layer is inserted between SiNx emitter and p-type Si anode to suppress the holes overflow in Si/SiN_x-based LEDs [17]. In addition, light-extraction efficiency was doubly enhanced by patterned SiNx-emitting layer grown on annealed Si film of dense nano cones [18].

In this work, a remarkable improvement of EL efficiency in SiN_x-based LED with aluminum-doped zinc oxide (AZO)/SiN_x/nc-Si/p-Si/Al multilayer structure were demonstrated by H₂ plasma treatment of nc-Si interlayer. Light emission efficiency was enhanced by more than 200% compared with LED without H₂ plasma treatment. High EL efficiency can be attributed to suppression of nonradiative recombination process. Improved performance of proposed LEDs was discussed in detail on basis of H₂ plasma treatment.

2. Experimental Details

The a-Si:H layer with thickness of 20 nm was first deposited on *p*-Si (100) wafers (2 Ωcm) and quartz in very high frequency plasma enhanced chemical vapor deposition system using mixture of SiH₄ and H₂ as reactant gas sources at flux ratio of 1.5:80. Upon growing, radio frequency (RF) power, chamber pressure, and substrate temperature were 30 W, 60 Pa, and 250 °C, respectively. After deposition, as-deposited films were first dehydrogenated at 400 °C and then annealed at 1100 °C in N₂ atmosphere for 30 min to transform ultrathin amorphous a-Si layer to crystalline. Subsequently, nc-Si films were exposed to RF-generated H₂ plasma under reaction pressure of 60 Pa for 20 and 60 min. H₂ gas flow rate was 30 sccm. For both processes, RF power and substrate temperature were maintained at 40 W and 250 °C, respectively. Afterward, 40 nm thick SiN_x film was grown on plasma-treated nc-Si layer by using H₂ and NH₃-diluted SiH₄ as precursor gases. Flow rates of SiH₄, NH₃, and H₂ were maintained at 5, 20, and 90 sccm, respectively. RF power, substrate temperature, and deposition pressure were fixed at 30 W, 250 °C, and 60 Pa, respectively. To fabricate LEDs, luminescent active layer was sputtered with dot-shaped AZO top electrode with diameter of 1.5 mm. Aluminum was evaporated on back of *p*-Si wafer surface. The SiN_x-based LEDs were designated as device_x(x = 0, 20, 60) with the H₂ plasma treatment time of 0, 20, and 60 min. Fig. 1 shows schematic structure of SiN_x-based LEDs. Raman spectroscopy and Fourier transform infrared spectroscopy (FTIR) was conducted to investigate microstructure and the bonding configurations of nc-Si films with H₂ plasma treatment at different treatment periods, respectively. Room-temperature EL spectra measurements were acquired on Jobin Yvon fluorolog-3 spectrophotometer.

3. Results

Fig. 2 shows EL spectra of SiN_x-based LEDs with and without H₂ plasma treatment under different forward biases. At around 760 nm, EL emission peak can be detected under low injected current

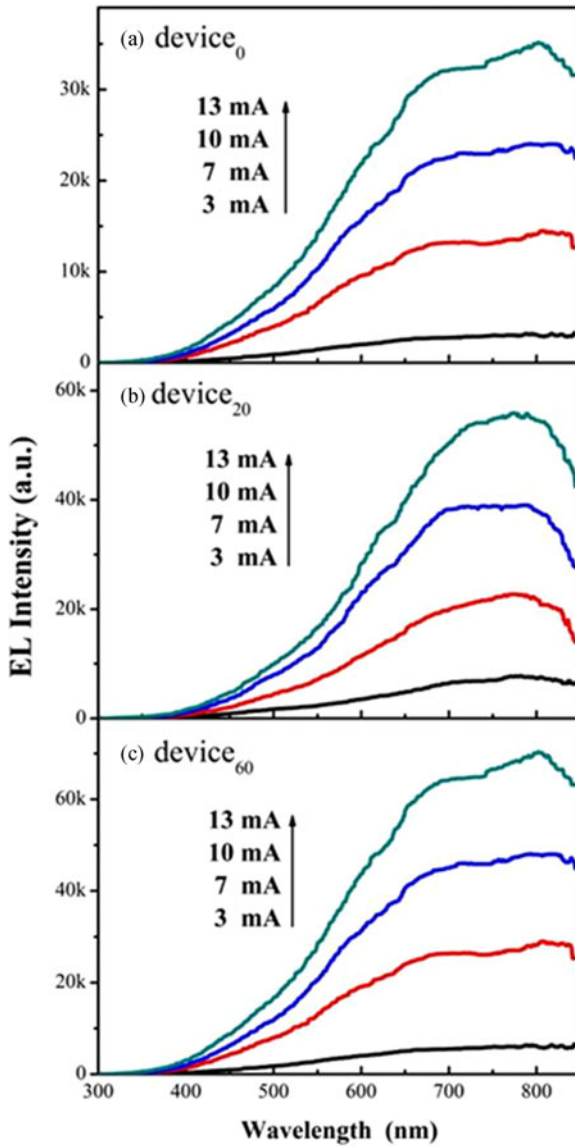


Fig. 2. EL spectra of the SiN_x -based LEDs (a) without H_2 plasma treatment, (b) with H_2 plasma treatment for 20 min, and (c) with H_2 plasma treatment for 60 min under different injected currents.

of 3 mA. As shown in Fig. 2, EL intensity of both SiN_x -based LEDs increase with increasing injected current. Interestingly, remarkably enhanced EL intensity is observed in SiN_x -based LEDs with H_2 plasma treatment in comparison with device without H_2 plasma treatment. Furthermore, by increasing H_2 plasma treatment time from 20 min to 60 min, EL intensity can be further improved at same injected current. This result indicates that enhancement of EL efficiency is significantly affected by H_2 plasma treatment of nc-Si interlayer. Fig. 3 shows the current-voltage curve of the devices with and without H_2 plasma treatment, respectively. It can be seen that the injected current of the devices with H_2 plasma treatment is significantly higher than that of the reference one under the same driving voltage. It means that the H_2 plasma treatment of nc-Si interlayer would result in an obvious decrease of the on-series resistance for the SiN_x -based LEDs in our case. From the inset of Fig. 3, it is also found that the current-voltage date from all the devices can well fitted by the $\ln(I)-E^{-1}$ relation, which demonstrates that the dominant conduction mechanism of our devices is Trap-assisted tunneling, as confirmed in our previous work.

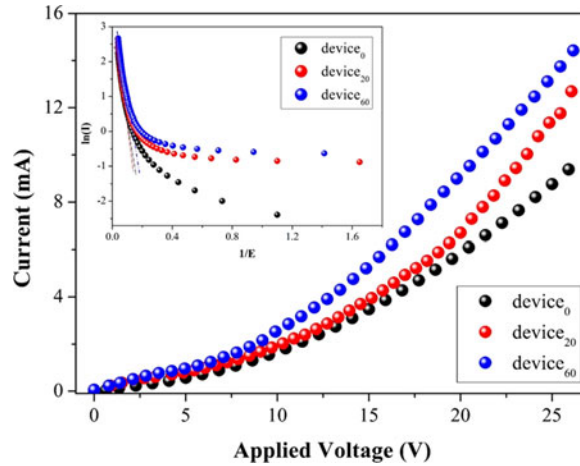


Fig. 3. Current-voltage characteristics of the SiN_x -based LEDs with and without H_2 plasma treatment, respectively. The inset shows the quantity $\ln(I)$ plotted as a function of E^{-1} for the devices with and without H_2 plasma treatment, respectively. E is in MV cm^{-1} .

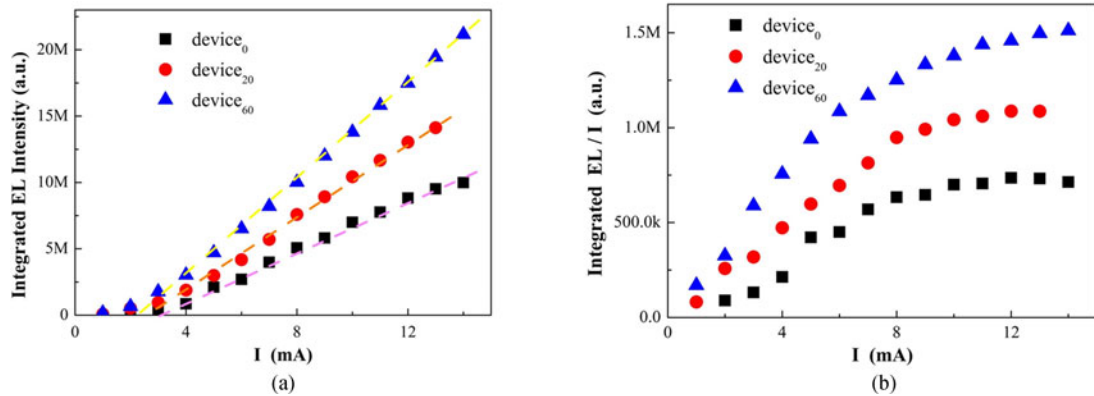


Fig. 4. The integrated EL intensity (a) and the ratio of the integrated EL intensity to the injected current (b) as the function of injected current for the devices with and without H_2 plasma treatment, respectively.

Fig. 4(a) shows integrated EL intensity of devices as function of injected current. EL intensity in both devices increased monotonically with increasing injected current. As shown in Fig. 4(a), integrated EL intensity of all devices show linear relation with injected current, implying that EL emission mainly resulted from recombination of bipolar injected electrons and holes [17]. Meanwhile, EL intensity from device₆₀ is much intensive at same injected current. Under injected current of 14 mA, EL intensity significantly increases by more than 200% compared with device₀ without H_2 plasma treatment. External quantum efficiency (EQE) of EL for LEDs is defined as ratio of output power (P) to injected current, where P value is proportional to integrated EL intensity. EQE of devices can be compared quantitatively by comparing ratio of integrated EL intensity to injected current under the same injected current, as shown in Fig. 4(b). Overall, EQE of devices with H_2 plasma treatment is remarkably enhanced compared with reference device₀, and increased EL efficiency by 200% is obtained by H_2 plasma treatment for 60 min at injected current of 14 mA. Moreover, as indicated in Fig. 4(b), EQE of reference device₀ degenerates gradually with further increase in injected current, and this phenomenon is possibly originated from Auger nonradiative recombination and/or carrier overflow [19]. This efficiency droop is overcome by H_2 plasma treatment of nc-Si interlayer. Improved EL characteristics in devices may be correlated with suppression of nonradiative recombination by H_2 plasma treatment of nc-Si interlayer.

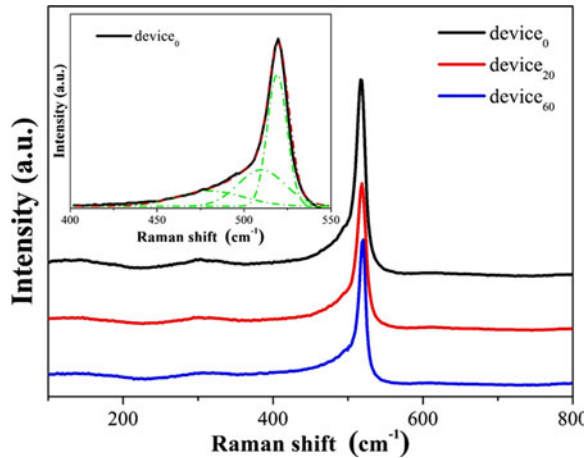


Fig. 5. Raman spectra of the inserted nc-Si layer with and without H_2 plasma treatment. (The spectra were deconvoluted into three Gaussian bands, centered at 480 cm^{-1} , 510 cm^{-1} , and 520 cm^{-1} , respectively. The deconvoluted peaks are shown as dashed lines.)

To understand improvement of EL efficiency of SiN_x -based LEDs, Raman spectroscopy was performed to examine microstructure of inserted nc-Si layer with and without H_2 plasma treatment. Results are shown in Fig. 5. Crystalline fraction X_c can be evaluated from Raman spectrum using the following equation:

$$X_c = \frac{I_c + I_m}{I_c + I_m + \beta I_a} \times 100\% \quad (1)$$

where β is constant related to crystalline to amorphous phase scattering cross section ratio of 0.8. I_c , I_m , and I_a are integrated intensities of crystalline Gaussian peak at around 520 cm^{-1} , intermediate Gaussian peak at around 510 cm^{-1} , and amorphous Gaussian peak at around 480 cm^{-1} , respectively [20]. For reference nc-Si layer, crystalline fraction X_c is 78.7%. After H_2 plasma treatment for 60 min, crystalline fraction X_c of nc-Si slightly increases to 83.6%, implying improvement in structural order of Si network. This phenomenon resulted from etching effect of hydrogen, which preferentially removes weak or strained Si-Si bonds [21]. However, the change in the crystalline fraction X_c of nc-Si from the film before and after the H_2 plasma treatment are quite small. Thus, it is considered that the improvement of EL efficiency may be not originated from the improvement in crystalline fraction of nc-Si layer.

The local bonding configurations of the nc-Si layers were further investigated by FTIR spectra, as shown in Fig. 6. The as-deposited a-Si:H film has the following vibrational absorption modes: the predominant absorption bands at 642 cm^{-1} and 2097 cm^{-1} are connected to the Si-H_n wagging mode and the H-Si-Si₂O stretching mode, respectively [22]. The 862 cm^{-1} band is ascribed to the H-SiO₃ bending mode [23]. In addition, the band located at 1035 cm^{-1} corresponds to the Si-O-Si stretching mode [23]. A remarkable feature of the FTIR spectra is that the signals of the H-Si related absorption bands are diminished after the films were annealed at 1100°C . This indicates that the Si-H bonds break, which would undoubtedly produce Si-related defects. After H_2 plasma treatment for 20 min, a weak absorption band located at 663 cm^{-1} , which is assigned to the Si-H_n wagging mode, can be observed. This absorption band significantly increases with increasing H_2 plasma treatment up to 60 min, as shown in Fig. 6. This obviously demonstrates that H_2 plasma treatment can facilitate Si-H bonds and thus passivate the Si-related defects. Therefore, the improved EL efficiency can be attributed to the hydrogen passivation, which effectively reduces Si-related defect state density in nc-Si interlayer.

The improvement of EL efficiency, $\ln(I) - \ln(P^{0.5})$ characteristics were also used to discuss dominant type of recombination in devices, as shown in Fig. 7. Theoretically, given the Boltzmann statistics of carrier and absence of leakage currents, injected currents (I) can be related to carrier density (n)

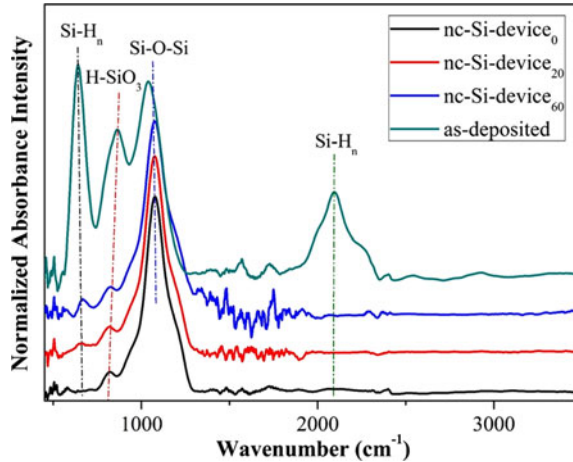


Fig. 6. FTIR spectra of the as-deposited a-Si:H film and the annealed nc-Si film with and without H₂ plasma treatment, respectively.

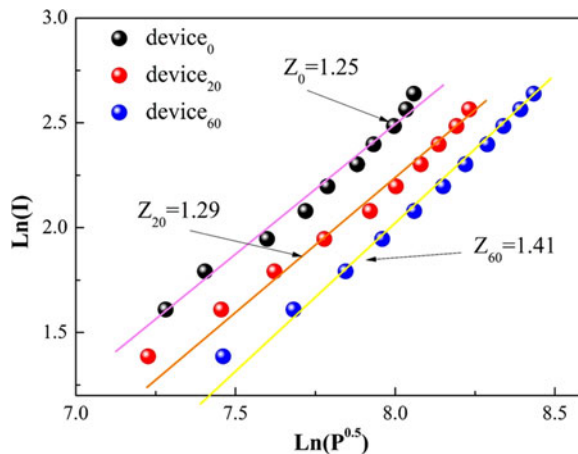


Fig. 7. Plots of ln(I) versus ln(P^{0.5}) for the devices with and without H₂ plasma treatment, respectively. The P is characterized indirectly by the integrated EL intensity. The Z parameters calculated from the linear fittings of ln(I) versus ln(P^{0.5}) for each curve are also provided.

in devices; related equation is as follows:

$$I = eV (A n + B n^2 + C n^3) \quad (2)$$

where e and V represent electronic charge and active volume in devices, respectively. A, B, and C are coefficient associated with nonradiative recombination, bimolecular radiative recombination, and Auger-related recombination, respectively [24], [25]. Assuming that current in devices originates from one of these recombinations, (2) can be transformed into the following format:

$$\ln(I) = Z \ln(P^{0.5}) + C \quad (3)$$

where C is constant [26]. In (3), the Z parameter may range from 1 to 3 for different recombination mechanisms in which the value of 1, 2 and 3 represent the nonradiative, the bimolecular radiative and the Auger dominated recombination process, respectively [17], [26]. Therefore, dominant recombination in devices can be identified by linearly fitting ln(P^{0.5}) versus ln(I). From Fig. 7, Z₀ value of 1.25 is obtained for reference device₀ without H₂ plasma treatment, indicating that nonradiative recombination is dominant process in devices. This result can be attributed in part to formation

of nonradiative recombination centers, such as Si dangling bonds at interface of nc-Si. After H₂ plasma treatment of inserted nc-Si layer, Z value increased to 1.41, indicating increased bimolecular radiative recombination rate in devices. Clearly, H₂ plasma treatment effectively reduces Si-related defect states in nc-Si interlayer, and thus suppressed nonradiative recombination in the device to some extent.

4. Conclusion

In summary, enhancement of EL efficiency was observed in SiN_x-based LED with AZO/SiN_x/nc-Si/p-Si/Al multilayer structure via H₂ plasma treatment of inserted nc-Si. Emission efficiency is significantly enhanced by more than 200% compared with device without H₂ plasma treatment. Moreover, the value of Z parameter from the device increases from 1.25 to 1.41 after H₂ plasma treatment of inserted nc-Si layer. Improved EL efficiency is attributed to suppression of nonradiative recombination, which resulted from the hydrogen passivation that effectively reducing Si-related defect state of the inserted nc-Si layer.

References

- [1] L. Pavesi, L. D. Negro, C. Mazzoleni, G. Franzo, and F. Priolo, "Optical gain in silicon nanocrystals," *Nature*, vol. 408, no. 6811, pp. 440–444, Nov. 2000.
- [2] A. Marconi, A. Anopchenko, M. Wang, G. Pucker, P. Bellutti, and L. Pavesi, "High power efficiency in Si-nc/SiO₂ multilayer light emitting devices by bipolar direct tunneling," *J. Appl. Phys.*, vol. 94, no. 22, Jun. 2009, Art. no. 221110.
- [3] G. R. Lin, C. J. Lin, C. K. Lin, L. J. Chou, and Y. L. Chueh, "Oxygen defect and Si nanocrystal dependent white-light and near-infrared electroluminescence of Si-implanted and plasma-enhanced chemical-vapor deposition-grown Si-rich SiO₂," *J. Appl. Phys.*, vol. 97, no. 9, Apr. 2005, Art. no. 094306.
- [4] L. Ding, M. B. Yu, X. Tu, G. Q. Lo, S. Tripathy, and T. P. Chen, "Laterally current injected light-emitting diodes based on nanocrystalline-Si/SiO₂ superlattice," *Opt. Exp.*, vol. 19, no. 3, pp. 2729–2738, Jan. 2011.
- [5] C. H. Cheng, Y. C. Lien, C. L. Wu, and G. R. Lin, "Multicolor electroluminescent Si quantum dots embedded in SiO_x thin film MOSLED with 2.4% external quantum efficiency," *Opt. Exp.*, vol. 21, no. 1, pp. 391–403, Jan. 2013.
- [6] W. Mu *et al.*, "Direct-current and alternating-current driving Si quantum dots-based light emitting device," *IEEE J. Sel. Topics Quantum Electron.*, vol. 20, no. 4, pp. 206–211, Apr. 2013.
- [7] G. R. Lin, C. L. Wu, C. W. Lian, and H. C. Chang, "Saturated small-signal gain of Si quantum dots embedded in SiO₂/SiO_x/SiO₂ strip-loaded waveguide amplifier made on quartz," *Appl. Phys. Lett.*, vol. 95, no. 2, Jul. 2009, Art. no. 021106.
- [8] G. R. Lin, C. W. Lian, C. L. Wu, and Y. H. Lin, "Gain analysis of optically-pumped Si nanocrystal waveguide amplifiers on silicon substrate," *Opt. Exp.*, vol. 18, no. 9, pp. 9213–9219, Apr. 2010.
- [9] N. M. Park, C. J. Choi, T. Y. Seong, and S. J. Park, "Quantum confinement in amorphous silicon quantum dots embedded in silicon nitride," *Phys. Rev. Lett.*, vol. 86, no. 7, pp. 1355–1357, Feb. 2001.
- [10] L. D. Negro, J. H. Yi, L. C. Kimerling, S. Hamel, A. Williamson, and G. Galli, "Light emission from silicon-rich nitride nanostructures," *Appl. Phys. Lett.*, vol. 88, no. 18, May 2006, Art. no. 183103.
- [11] R. Huang *et al.*, "Role of barrier layers in electroluminescence from SiN-based multilayer light emitting devices," *Appl. Phys. Lett.*, vol. 92, no. 18, May 2008, Art. no. 181106.
- [12] R. Huang *et al.*, "Origin of strong white electroluminescence from dense Si nanodots embedded in silicon nitride," *Opt. Lett.*, vol. 37, no. 4, pp. 692–694, Feb. 2012.
- [13] F. Wang, D. Li, D. Yang, and D. Que, "Enhancement of light-extraction efficiency of SiN_x light emitting devices through a rough Ag island film," *Appl. Phys. Lett.*, vol. 100, no. 3, Jan. 2012, Art. no. 031113.
- [14] X. Wang, R. Huang, C. Song, Y. Guo, and J. Song, "Effect of barrier layers on electroluminescence from Si/SiO_xN_y multilayer structures," *Appl. Phys. Lett.*, vol. 102, no. 8, Feb. 2013, Art. no. 081114.
- [15] G. R. Lin, Y. H. Pai, C. T. Lin, and C. C. Chen, "Comparison on the electroluminescence of Si-rich SiN_x and SiO_x based light-emitting diodes," *Appl. Phys. Lett.*, vol. 96, no. 26, Jul. 2010, Art. no. 263514.
- [16] C. D. Lin, C. H. Cheng, Y. H. Lin, C. L. Wu, Y. H. Pai, and G. R. Lin, "Comparing retention and recombination of electrically injected carriers in Si quantum dots embedded in Si-rich SiN_x films," *Appl. Phys. Lett.*, vol. 99, no. 24, Dec. 2011, Art. no. 243501.
- [17] R. Huang *et al.*, "Suppression of hole overflow and enhancement of light emission efficiency in Si quantum dots based silicon nitride light emitting diodes," *IEEE J. Sel. Topics Quantum Electron.*, vol. 20, no. 4, Aug. 2014, Art. no. 8200306.
- [18] Y. Guo *et al.*, "Efficiency enhancement for SiN-based light emitting device through introduction of Si nanocones in emitting layer," *Opt. Mater. Exp.*, vol. 5, no. 5, pp. 969–976, May 2015.
- [19] D. Li, J. Huang and D. Yang, "Enhanced electroluminescence of silicon-rich silicon nitride light-emitting devices by NH₃ plasma and annealing treatment," *Physica E*, vol. 41, no. 6, pp. 920–922, May 2009.
- [20] C. Song *et al.*, "Structural and electronic properties of Si nanocrystals embedded in amorphous SiC matrix," *J. Alloys Compd.*, vol. 509, no. 9, pp. 3963–3966, Mar. 2011.

- [21] P. Dutta, S. Paul, D. Galipeau, and V. Bommisetty, "Effect of hydrogen plasma treatment on the surface morphology, microstructure and electronic transport properties of nc-Si:H," *Thin Solid Films*, vol. 518, no. 23, pp. 6811–6817, Sep. 2010.
- [22] Y. Rui *et al.*, "Effects of hydrogen plasma annealing on the luminescence from a-Si: H/SiO₂ and nc-Si/SiO₂ multilayers," *Appl. Surf. Sci.*, vol. 253, no. 21, pp. 8647–8651, Aug. 2007.
- [23] K. Chen *et al.*, "Comparison between light emission from Si/SiN_x and Si/SiO₂ multilayers: Role of interface states," *J. Non-Cryst. Solids*, vol. 338, pp. 448–451, Jun. 2004.
- [24] C. H. Cheng, C. L. Wu, C. C. Chen, L. H. Tsai, Y. H. Lin, and G. R. Lin, "Si-rich light-emitting diodes with buried Si quantum dots," *IEEE Photon. J.*, vol. 4, no. 5, pp. 1762–1775, Oct. 2012.
- [25] A. J. Bennett, P. N. Stavrinou, C. Roberts, R. Murray, G. Parry, and J. S. Roberts, "A comparative study of spontaneous emission and carrier recombination processes in InGaAs quantum dots and GaInNAs quantum wells emitting near 1300 nm," *J. Appl. Phys.*, vol. 92, no. 10, pp. 6215–6218, Oct. 2002.
- [26] F. Wang, D. Li, L. Jin, D. Yang, and D. Que, "Reduction of the efficiency droop in silicon nitride light-emitting devices by localized surface plasmons," *Appl. Phys. Lett.*, vol. 102, no. 8, Feb. 2013, Art. no. 081108.